Physics of the Earth and Planetary Interiors 190–191 (2012) 80–86

Contents lists available at SciVerse ScienceDirect

Physics of the Earth and Planetary Interiors

journal homepage: www.elsevier.com/locate/pepi

Single-crystal elasticity of stishovite: New experimental data obtained using high-frequency resonant ultrasound spectroscopy and a Gingham check structure model

Akira Yoneda [a,*], Titus Cooray [a,1], Anton Shatskiy [b,c]

[a] Institute for Study of The Earth's Interior, Okayama University, Misasa, Tottori 682-0193, Japan
[b] Department of Earth and Planetary Material Science, Graduate School of Science, Tohoku University, Sendai 980-8578, Japan
[c] V.S. Sobolev Institute of Geology and Mineralogy, SB RAS, Novosibirsk 630090, Russia

ARTICLE INFO

Article history:
Received 7 August 2011
Received in revised form 26 November 2011
Accepted 28 November 2011
Available online 3 December 2011
Edited by Kei Hirose

Keywords:
Stishovite
Elasticity
Bulk modulus
Acoustic velocity
Resonant ultrasound spectroscopy
Finite element method

ABSTRACT

Single-crystal elasticity of stishovite was examined using a new experimental technique and an empirical macroscopic model. Employing high-frequency resonant ultrasound spectroscopy, single-crystal elastic constants of stishovite were determined: C_{11} = 443(3), C_{33} = 781(4), C_{12} = 193(2), C_{23} = 199(2), C_{44} = 256(2), and C_{33} = 316(2) GPa. The frequency range of the resonant ultrasound spectroscopy techniques was 6–20 MHz, which is much lower than the ~10 GHz range of the Brillouin scattering technique. Of the elastic constants, the shear elastic constants C_{44} and C_{66} are consistent with the average value of the previously mentioned Brillouin scattering. Conversely, the four elastic constants, C_{11}, C_{33}, C_{12}, and C_{23}, slightly deviate outside the range of previous Brillouin scattering results. The present results, except those for C_{12}, are consistent with recent lattice dynamic analysis of inelastic X-ray scattering data. The adiabatic bulk modulus was calculated as 298 GPa, which is smaller and more consistent with the result of compression experiments than any other Brillouin scattering results (301–312 GPa). The present result shows greater P-wave velocity anisotropy (24.7%) than any preceding work. To understand the unique elastic properties of stishovite, the Gingham check model was proposed and examined. The result shows that the octahedron of 6-coordinated Si in stishovite crystal has stiffness comparable to that of diamond.

1. Introduction

Stishovite is one of the most remarkable minerals in mineralogy, petrology, and geology. It was synthesized in 1961 (Stishov and Popova, 1961), and soon after discovered in a meteor impact crater in 1962 (Chao et al., 1962). It is one of the high-pressure polymorphs of SiO_2 with unique crystal structure, or, rutile structure (e.g., Smyth and Swope, 1993). It is believed to exist in the subduction slab between 300 and 1500 km depth (e.g., Irifune and Ringwood, 1993; Ono et al., 2001; Ricolleau et al., 2010). It is attracting further attention because of its high ultrasonic wave velocities and large elastic anisotropy. In the present study, we examined the single-crystal elasticity of stishovite through experiment and empirical modeling.

Single-crystal elastic constants of stishovite have been measured three times by means of the Brillouin scattering (BLS) technique (Weidner et al., 1982; Brazhkin et al., 2005; Jiang et al., 2008). Weidner et al. were first to determine all the single-crystal elastic constants of a high-pressure mineral using this method. Subsequently, the BLS technique became the standard technique for measuring the elasticity of high-pressure minerals. Brazhkin et al. (2005) performed high-temperature measurements of the amorphization temperature in stishovite (~830 K), and Jiang et al. (2008) conducted high-pressure experiments up to 22 GPa to examine shear softening in stishovite. Recently, the BLS technique has been successfully applied to lower mantle material under high pressures exceeding 100 GPa in a diamond anvil cell (e.g., Murakami et al., 2009).

The inconsistency in the BLS results for stishovite under ambient conditions, however, is as much as 5–6% for some elastic constants. Additionally, the reliability and accuracy of the BLS technique for high-pressure minerals still needs to be confirmed using another technique.

With this background, Yoneda et al. (2007) recently developed high-frequency resonant ultrasound spectroscopy (HFRUS) for a submillimeter specimen; this is an advanced development of resonant ultrasound spectroscopy (Ohno, 1976; Maynard, 1996; Migliori and Maynard, 2005) toward the higher frequency range (~50 MHz). We applied HFRUS to a single crystal stishovite to obtain a new set of elastic constants to compare with those hitherto obtained by BLS.

* Corresponding author.
E-mail address: yoneda@misasa.okayama-u.ac.jp (A. Yoneda).
[1] Present address: Department of Science and Technology, Uva Wellassa University, Badulla 90000, Sri Lanka.

0031-9201/$ - see front matter © 2011 Elsevier B.V. All rights reserved.
doi:10.1016/j.pepi.2011.11.003

The principal aim of this study was to demonstrate the performance of HFRUS by measuring a single-crystal specimen of stishovite as the first test sample among representative high-pressure phases. Additionally, we examined a macroscopic model to characterize the single-crystal elasticity of stishovite on the basis of its unique crystal structure, or Gingham check pattern.

2. Experimental

Fig. 1 shows a cross section of the cell assembly for the single-crystal growth of stishovite in a Kawai-type high-pressure apparatus. The edge lengths of the anvil truncation and octahedron were 11 and 18 mm, respectively. A single crystal of quartz was enclosed in a Pt capsule with water. The details of the crystal growth of stishovite have previously been reported by Shatskiy et al. (2010).

We grew a large single crystal of stishovite using a slow-cooling method starting at 12 GPa and 1400 °C. Fig. 2a is a photograph of a single crystal grain. Through characterization with a polarized microscope, micro-focus X-ray diffraction, and FTIR spectroscopy, we confirmed that the specimen was a single grain of pure stishovite with ~7 wt. ppm water content, which is reasonable water content for aluminum-free stishovite (Bolfan-Casanova et al., 2000; Litasov et al., 2007).

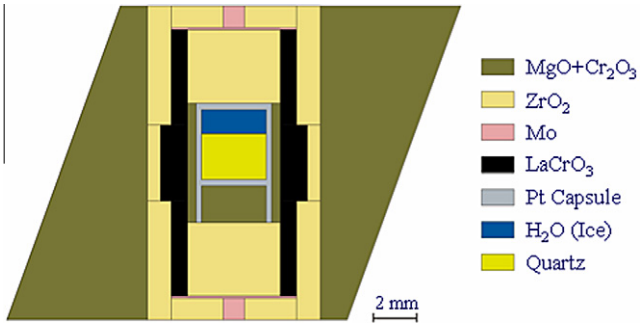

Fig. 1. Cross section of the cell assembly for the single-crystal growth of stishovite.

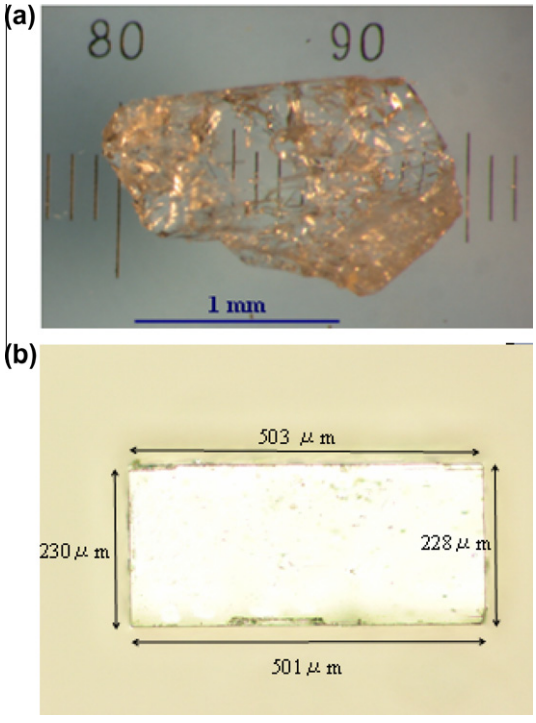

Fig. 2. (a) Photograph of a single crystal grain of stishovite synthesized in this study. (b) After shaping to a rectangle, the longest-edge direction is along the *c*-axis and the other directions are along the *a*-axis.

The specimen was shaped to a rectangle (229(1) × 288(1) × 502(1) μm) by manually polishing after determining the crystallographic orientation three times (Fig. 2b). All surfaces were polished with a 1 μm diamond paste as the final process.

Although the HFRUS technique was detailed by Yoneda et al. (2007), we present a brief introduction in the Appendix.

3. Results and discussion

Twenty peaks were detected and identified between 6 and 20 MHz as listed in Table 1. It is noted that the present frequency range is approximately twice the previous highest frequency range of ~10 MHz (Aizawa et al., 2004) owing to the development of the handmade transducer (Yoneda et al., 2007).

The remaining task was to find the most reasonable set of six independent elastic constants for the stishovite. For the density of stishovite, we used 4290 kg/m^3, following Weidner et al. (1982). Forward analyses of eigenfrequencies were conducted by means of the xyz method (Visscher et al., 1991; Yoneda, 2000). The mode classification based on the symmetry of the vibration pattern is presented in Table 2.

Table 3 shows derivatives of resonance frequency with respect to elastic constants for some selected modes. The first two A_u

Table 1
List of 20 peaks between 6 and 20 MHz. The grouping is based on the symmetry of the vibration pattern (see Table 2). Observed frequencies are shown together with frequencies calculated using the elastic constants determined in this study and listed in Table 5.

No.	Group	Observed frequency, Hz	Calculated frequency
1	$1A_u$	6791050	6831007
2	$1B_{2u}$	7659850	7655949
3	$1B_{1u}$	8475580	8494870
4	$1A_g$	11887800	11891607
5	$1B_{2g}$	12777000	12764877
6	$2B_{2u}$	12979700	13037821
7	$1B_{1g}$	13316400	13328523
8	$1B_{3u}$	13890600	13859754
9	$2A_g$	13906600	13885604
10	$3A_g$	14551800	14572214
11	$1B_{1g}$	14877200	14820279
12	$2A_u$	16608500	16598139
13	$2B_{3u}$	16735000	16720927
14	$2B_{1u}$	17587500	17497892
15	$3B_{2u}$	17794800	17858911
16	$4A_g$	18008000	18018687
17	$2B_{2g}$	18014000	18041523
18	$3B_{2g}$	18680000	18757086
19	$4B_{2u}$	18890000	18856408
20	$3B_{3u}$	19190000	19174234

Table 2
List of symbols for classifying the vibration mode. This system is used in the molecular vibration study. Plus '+' and minus '−' specify symmetry and antisymmetry along with *x*, *y*, and *z* directions.

Symbol	Symmetry
A_g	+++
B_{1u}	−++
B_{2u}	+−+
B_{3u}	++−
B_{1g}	+−−
B_{2g}	−+−
B_{3g}	−−+
A_u	−−−